Active filter harmonic compensator with proportional resonant current controller for photovoltaic inverter

Le Khoa Nam, Le Hong Lam, Trinh Trung Hieu, Nguyen Huu Hieu
Faculty of Electrical Engineering, The University of Danang–University of Science and Technology, Danang, Vietnam

Article Info	ABSTRACT
	The strong development of renewable energy sources (RES), especially distributed energy sources, brings many benefits to the power system. Single-phase photovoltaic (PV) systems are the fastest growing type of distributed energy source worldwide today. Besides the beneficial factors for the distribution power system, the high penetration rate of solar power systems also causes negative impacts, especially power quality issues. PV inverters generate harmonics during the high-frequency switching of semiconductor elements. Traditionally available passive filters are not effective enough to ensure output power quality when the PV system generates power to the distribution grid. Therefore, this study presents the design of a proportional resonant current controller combined with active filter harmonic compensated (PR+HC) for a single-phase PV inverter. This controller, when integrated into traditional PV inverter, will provide better output power quality, contributing to reducing total harmonic distortion (THD) on the distribution grid. This study analyzes the parameters affecting the harmonic attenuation effect of the PR+HC controller, then simulates it on MATLAB Simulink to evaluate the results. The results of the study show that the PR+HC controller is not only effective in reducing the amplitude of odd harmonics, but also operates reliably even when the grid frequency fluctuates widely.

Corresponding Author:

Trinh Trung Hieu
Faculty of Electrical Engineering, The University of Danang–University of Science and Technology
54 Nguyen Luong Bang, Danang, Vietnam
Email: tthieu@dut.udn.vn

1. INTRODUCTION

Distributed energy resources (DER) are being developed vigorously to meet the increasing energy demand. DER are typically renewable energy sources (RES) such as solar, wind or small hydropower. Among them, photovoltaic (PV) occupies a large share of the distributed power category because of its advantages in performance, reliability, and affordability. Single-phase PV inverters grid-connected are commonly used systems that contain i) DC/DC boost converters that perform maximum-power-point tracking control and voltage amplification and ii) DC/AC inverter which responsible for power quality, equipment protection and synchronous grid-current injection. Various PV module orientations and technologies can be integrated thanks to this adaptable design [1]–[4]. When connected to the grid, PV inverters must ensure the international standards specified by each grid (e.g., IEC 61727). They are required to comply with the requirements of power quality, fault ride through and the ability of anti-islanding when there is a blackout. PV inverters must comply with specific criteria regarding voltage, frequency and generated harmonics to ensure satisfactory power quality [5], [6].

Power quality is one of the most concerned issues when RES integrated into the power system [7]–[10]. The harmonics of the PV system are mainly generated from the power electronic inverter. It consists of high-frequency switching semiconductor devices and injects these high-frequency harmonic current components (also known as super-harmonic) into the grid. This amount of harmonics has a negative impact on the power system, causing transient, instability, increase transformer and conductor loss [11]. According to Digalovski *et al.* [12], the distribution system has a total harmonic distortion (THD) of the grid voltage of about 10%, transformers can suffer from 2% to 15% losses, generators can suffer from 6% losses, and capacitor losses can range from 15% to 16%. Even though PV inverters have provisions to control the level of harmonics generated, when there is a high level of PV penetration, the THD of the grid is still exceeded. At the same time, although the current controller has a high sinusoidal reference monitoring ability, the output current of the grid-connected PV inverter always has a certain distortion. In cases where DER penetration level increases above the system's hosting capacity, the harmonics they create can degrade the overall power quality of the power distribution system. Similarly, the level of harmonic pollution is high at the point of common coupling (PCC), the hosting capacity of the system is reduced and the grid cannot absorb the maximum DER potential [13]–[15].

Due to the current controller's crucial role in ensuring high-quality sinusoidal output from the PV inverter to the grid, precise design is imperative to minimize harmonics. Based on linear current control, a proportional integral (PI) controller is proposed for application [16]. Despite its simplicity, this structure has considerable drawbacks in terms of phase and amplitude errors in steady state. Although high control gain can reduce steady-state errors, this is not a practical solution due to increased disturbance and probable instability [17]. Another drawback of the modified PI controller is the potential for current distortion as a result of background harmonics created in the internal circuit when the grid voltage is distorted [18]. Proportional resonant (PR) current control is proposed as an alternative to the conventional PI controller used in DC/AC inverters [19]–[21]. The PR controller provides superior performance in both reference tracking and noise reduction, thereby decrease steady-state error [22]–[25]. PR current controller is widely used in studies on minimizing harmonics from PV systems [26], [27].

There are many studies on eliminating harmonics from DER to facilitate their sustainable development in distribution power systems [28]–[30]. Some studies propose active filters that not only compensate for harmonics generated by distorted and fluctuating loads but also mitigate harmonics generated from the DER itself [31]–[35]. He *et al.* [33] proposed a controller for DER with the goal of ancillary harmonic compensation (HC) for local non-linear load and in case of frequency disturbance. The system is equipped with two effectively independent control branches. The first branch oversees the fundamental current control of the DER unit, while the second branch is dedicated to compensating for local load harmonic current or feeder resonance voltage. The results of the study show that in the case of local load harmonic current, the THD of current grid is reduced from 41.73% to 3.64%; in case of feeder resonance voltage, THD of PCC voltage decreased from 17.03% to 5.25%. However, this study has not performed analyzes to select parameters for the harmonic controller. Furthermore, there is no mention of addressing the reduction of harmonics generated by the DER itself. By specifically addressing the minimization of harmonics from DERs, which serve as the primary contributors to harmonic distortion, it ensures that the THD remains within acceptable limits across the distribution power system. With that philosophy, research [35] proposed a model combining PR current controller and harmonic compensator (HC) with many parallel blocks for single-phase PV inverter grid-connected. The HC resonator is designed to compensate for odd-order harmonics emitted from the PV inverter itself. Simulation and experimental results with a 2 kWp PV system show that the output power quality of the inverter is greatly improved. The odd-order current harmonics from the PV inverter output were all reduced to below 0.4%. However, a limitation of this study is that the parameters of PR and HC are chosen based on experience without going through any analysis.

Based on the limitations of previous research and the advantages of PR controller and HC active filter, this paper proposes to design a PR+HC controller for single-phase PV inverters to compensate for odd harmonics generated by itself. The selective HC are connected in series and all are connected in parallel to the PR current controller. MATLAB Simulink is used to simulate the model. The obtained harmonic analysis results and bode diagrams are generated with this software [36]. The contributions of this study include:
- Building a model of a grid-connected single-phase PV system integrating PR+HC system to minimize generated harmonics. Test the operation of this model using the reliable software MATLAB Simulink;
- Analyzing the effects of PR and HC parameters to select appropriate values for each harmonic filter element in this system. This is an aspect that is often not mentioned much in research on harmonic suppression controllers;
- Evaluating the output power quality of PV inverter in case of missing and complete PR+HC active filter blocks;
- Evaluating the stable working ability of PR+HC in case of frequency fluctuations.

There are five sections in this study. The structure of PV inverter including LCL filter, the PR controller and the resonant HC system are introduced in section 2. Section 3 describes the parameters of the aforementioned systems as they apply to the 2 kWp single-phase PV inverter grid-connected. Section 4 delves into the simulation results, detailing their implications, while section 5 summarizes the conclusions drawn from the study.

2. LCL FILTER, CURRENT CONTROLLER AND HARMONIC COMPENSATORS
2.1. LCL filter

Figure 1 presents the model of single-phase PV inverter grid-connected. To decrease harmonics generated by the DC/AC converter, the power circuit contains an LCL filter. Even at low L and C values, the LCL filter can provide quite good harmonic attenuation ratios. The damping resistor R_d is connected in series in the branch of the capacitor circuit C_f to increase stability and reduce resonance. This system is called a passive damping filter. The use of both the PR+HC active filter and the LCL passive filter further enhances the suppression of harmonics generated by the inverter. The transfer function of the LCL filter is given by (1):

$$G_F(s) = \frac{R_d C_f s + 1}{L_i L_g C_f s^3 + (L_i + L_g) R_d C_f s^2 + (L_i + L_g) s} \tag{1}$$

The filter's resonant frequency is determined by:

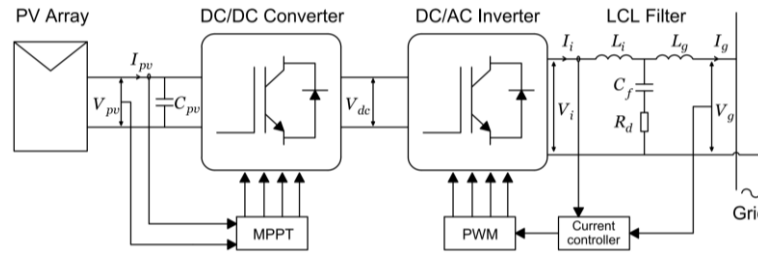$$\omega_{res} = \sqrt{\frac{L_i + L_g}{L_i L_g C_f}} \tag{2}$$

Figure 1. Single-phase PV inverter grid-connected model

2.2. PR current controller

Figure 2 presents the PR current controller scheme, where I_i is the current output of the inverter, I_{ref} is the current reference, V_{ref} is the voltage reference and I_{grid} is the output current of the inverter after the LCL filter. In addition, $G_F(s)$ represents the LCL filter. $G_D(s)$ is the transfer function of the PV inverter. This includes $G_P(s)$ is the transfer function of the PWM module and $G_d(s)$ is the control processing delay. For high switching frequency, the PWM module $G_P(s)$ can be modeled by a simple gain which is determined by (3). The control processing delay $G_d(s)$ is the delay time of one sampling period in PWM module defined by (4):

$$G_P(s) = \frac{V_{dc}}{V_m} \tag{3}$$

$$G_d(s) = e^{-T_d s} \tag{4}$$

where V_m and T_d denote the magnitude of the PWM triangular signal and the latency period of one sampling cycle, respectively. PR control is responsible for monitoring the reference signal. It is made up of a damped generalized integrator that has been set to resonate at the grid frequency f_0. The PR current controller is divided into two types: ideal and non-ideal, which are represented by (5) and (6), respectively:

$$G_{PR}(s) = K_p + K_i \frac{s}{s^2 + \omega_0^2} \tag{5}$$

$$G_{PR}(s) = K_p + K_i \frac{s}{s^2 + 2\omega_c s + \omega_0^2} \tag{6}$$

where K_p is the proportional gain term, K_i is the integral gain term and $\omega_0 = 2\pi f_0$ is grid frequency and ω_c is cutoff frequency.
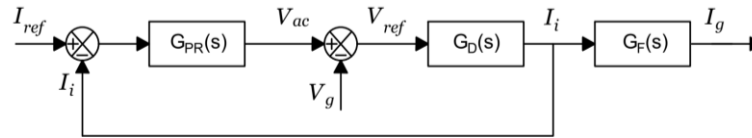
Figure 2. The PR current control block

The study conducts a comparative simulation of both ideal and non-ideal PR controllers, each with the same parameter of $K_p = 1$, $K_i = 100$ and $\omega_c = 1$ rad/s. The Bode diagram results are presented in Figure 3(a) for the ideal controller and Figure 3(b) for the non-ideal controller. In contrast to the ideal PR controller depicted in (5), which has infinite gain at the fundamental frequency ω_0 and exhibits no phase or gain deviations at other frequencies, the non-ideal PR controller in (6) offers a more practical approach. Its gain is finite, although it is still rather high for imposing minor steady-state errors. The ω_c components in (6) broaden the bandwidth, reducing sensitivity to grid frequency fluctuations and facilitating easier implementation in digital systems. Consequently, this study utilizes a non-ideal PR controller for a single-phase PV inverter grid-connected. It is clear from (6) that the design of the PR controller is dependent on the values of three parameters: K_p, K_i and ω_c. To investigate the influence of these parameters, the study simply assumes that any two parameters are constant and examines the effect of changes in the remaining parameters through Bode diagram.

- For the case $K_p = 0$ and $\omega_c = 1$ rad/s, the change of K_i affects only the gain of the PR controller, not the bandwidth. It can be shown that as K_i increases, the magnitude of the PR controller also increases. Base on this analysis, employing a high K_i value is suitable for achieving substantial attenuation of current harmonics. The Bode diagram of this case is shown in Figure 4(a);

- For the case $K_p = 0$ and case $K_i = 1$ the change of ω_c affects both the magnitude and the phase of the PR controller. The magnitude and phase increase as ω_c increases, but every ω_c peaks at the same resonant frequency of the controller. The resonance peak will be smaller and the filter more sensitive to frequency fluctuations with a lower ω_c. This also results in a slower transient response. Thus, according to research [18], ω_c should be chosen from 5-15 to obtain a compromise. The Bode diagram of this case is shown in Figure 4(b);

- For the case $K_i = 1$ and $\omega_c = 1$ rad/s, when K_p is added, the magnitude of the PR controller grows and reaches a peak at the resonant frequency, while the magnitude of the phase decreases. Based on the diagram, modest K_p values are preferable for obtaining adequate bandwidth to accommodate the other HC while maintaining system stability. The Bode diagram of this case is shown in Figure 4(c).

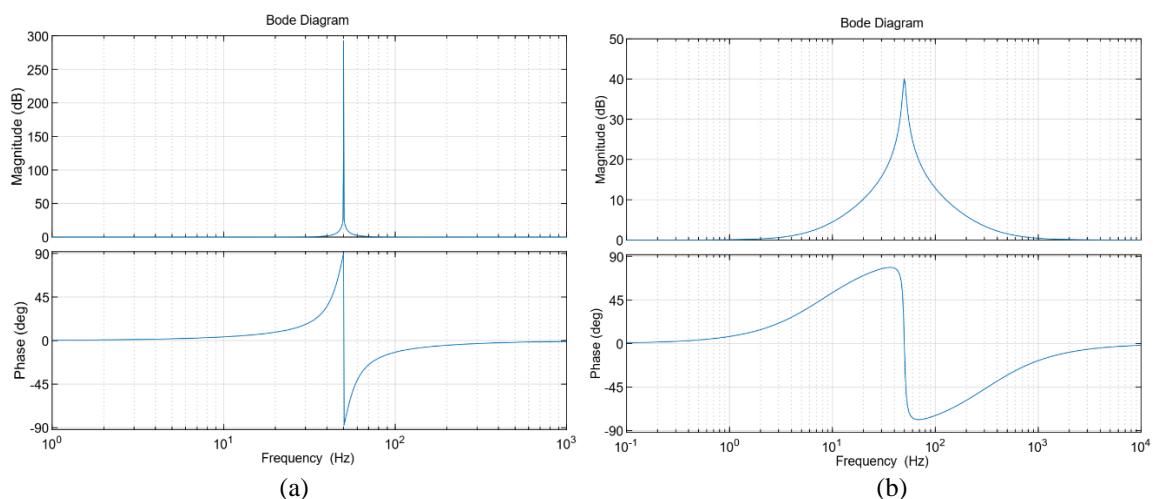
(a)   (b)

Figure 3. The PR controller block single-phase PV inverter grid-connected model frequency responses of; (a) ideal and (b) non-ideal PR controller with $K_p = 1$, $K_i = 100$ and $\omega_c = 1$ rad/s
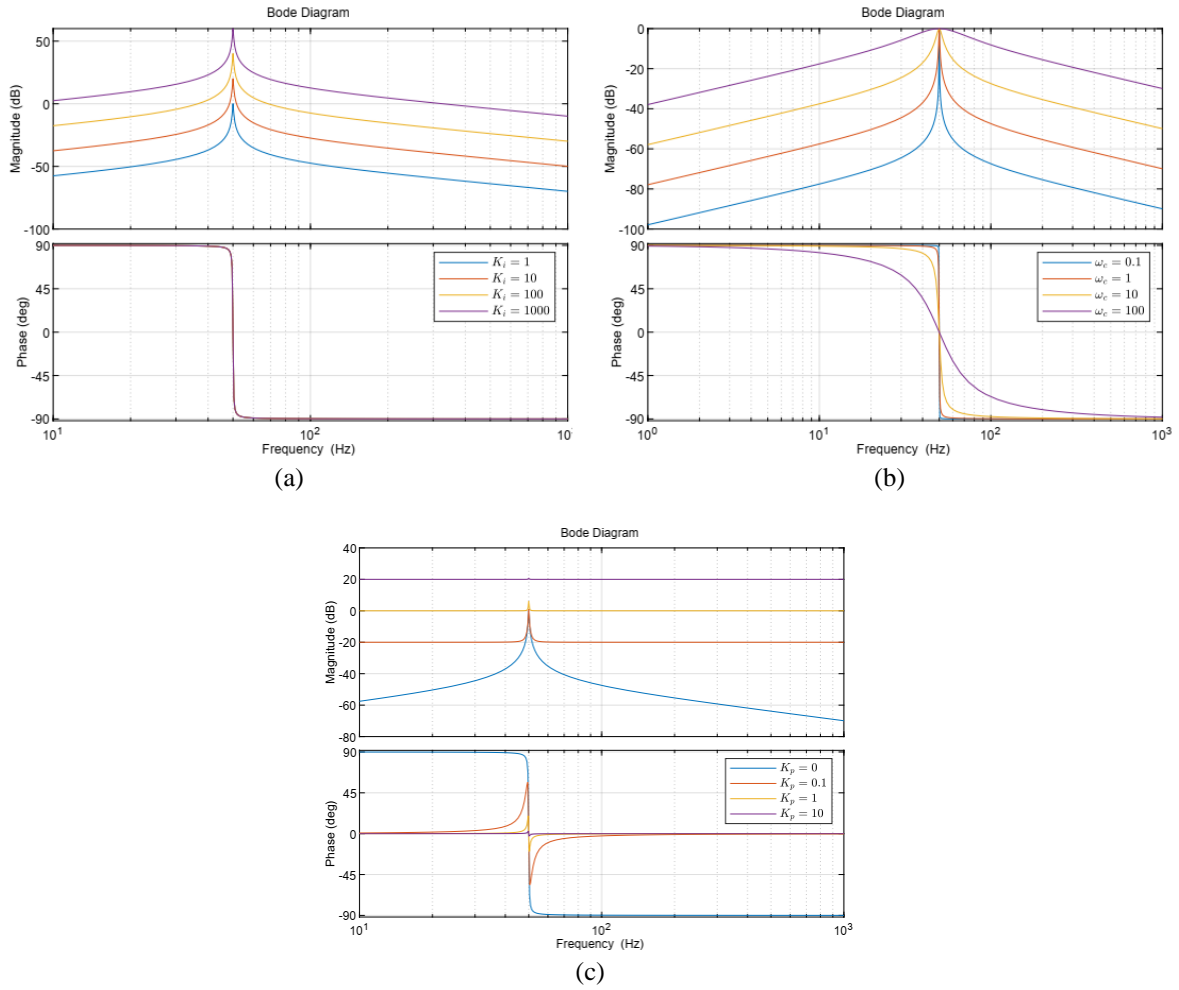
Figure 4. Frequency responses of non-ideal PR controller when; (a) K_i changes, (b) ω_c changes, and (c) K_p changes

2.3. PR current controller and HC

Figure 5 shows the control diagram of PR current controller combined with HC, which represented by block $G_{HC}(s)$. The ideal HC is represented by (7):

$$G_{HC}(s) = \sum_{h=3,5,7,\dots} K_{ih} \frac{s}{s^2+(h\omega_0)^2} \tag{7}$$

where h is the harmonic order to be compensated for, K_{ih} is the individual resonant gain at the harmonic h and $h\omega_0$ is the resonant frequency of the harmonic h. Because of the infinite gain, the ideal HC, like the ideal PR control, can cause stability issues. To circumvent this issue, the HC can be turned into a non-ideal by using (8). The HC gain at harmonic frequency h is still sufficient for compensation in the same case as the fundamental PR controller (see Figure 6). This research utilizes a non-ideal HC for a single-phase PV inverter grid-connected.

$$G_{HC}(s) = \sum_{h=3,5,7,\dots} K_{ih} \frac{2\omega_c s}{s^2+2\omega_c s+(h\omega_0)^2} \tag{8}$$

where, ω_c is the bandwidth around the harmonic frequency of $h\omega_0$.

The principal function of the HC system is to suppress odd harmonics with significant amplitudes, such as the 3rd, 5th, and 7th harmonic frequencies. According to (8), the HC system is mainly determined by two factors, ω_c and K_{ih}. It is necessary to fine-tune these two parameters for the compensator to achieve optimal operation. For the cut frequency ω_c, choosing it uniformly is best suited to obtain low bandwidth for effective selective HC. This is also true because the harmonic regions adjacent to the 3rd, 5th, and 7th

harmonic frequencies have very small widths. Figure 6 shows the resonance peaks of the HC unit at selected frequencies of 150 Hz, 250 Hz and 350 Hz. In this figure, ω_c uniformly has a smaller value, indicating that the resonance peaks are narrower. This improves the compensator's selectivity with predefined harmonics. However, a too low ω_c value can cause the HC to work inefficiently when the fundamental frequency changes. In addition, a low ω_c value makes it difficult to make the HC implementation as a digital system. On the other hand, the parameter K_{ih} represents the individual resonance gain, similar to the PR controller. It should be sufficiently large to induce minimal steady-state error while avoiding destabilization of the entire system. As the value of h increases, the amplitude of the harmonics will become smaller, so K_{ih} may not need to be selected uniformly. Parameter K_{i3} can be selected with high value and decreasing for K_{i5} and K_{i7}.
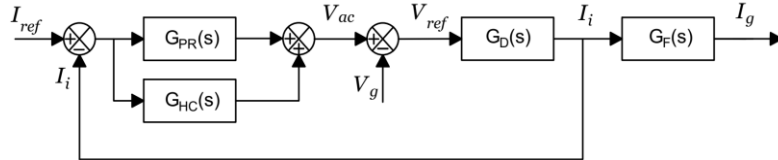
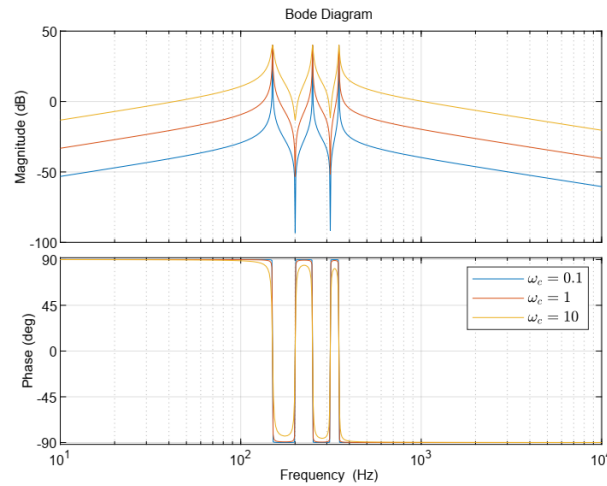

Figure 5. The PR controller and HC block

Figure 6. Block HC with $K_{ih} = 100$ and ω_c changes

3. LCL FILTER AND CURRENT CONTROLLER DESIGNATION

3.1. PV inverter and LCL filter parameters

This study uses a single-phase 2 kWp PV system to test the PR+HC system. The parameters of LCL filter are as follows: inverter-side filter inductor $L_i = 5$ mH; grid-side inductor $L_g = 2.8$ mH; filter capacitor $C_f = 5$ μC; filter damping resistor $R_d = 0.5$ Ω; switching frequency is 2 kHz. The grid voltage (RMS) is 380 V with the normal frequency f_0 is 50 Hz. DC bus voltage reference is 400 V. V_m is PMW triangular signal amplitude and set to 400 V and computational delay of PWM $T_d = 50$ μs.

3.2. PR controller parameters

According to the analysis outlined in section 2.2, the study selects the parameters for the design of PR current controller as follows: $K_p = 10$, $K_i = 200$ and $\omega_c = 1$ rad/s. The transfer function is represented as (9):

$$G_{PR}(s) = 10 + 200 \frac{2s}{s^2 + 2s + (2\pi 50)^2} \tag{9}$$

Open-loop and closed-loop bode diagrams are shown in Figures 7(a) and (b) to evaluate the stability of the PR controller. This control system has only PR controller and no HC (system in Figure 2). By the

function of MATLAB, the closed-loop is determined to be stable with the gain margin obtained is 39.4 dB at a frequency of 1150 Hz and the phase margin obtained is 24.5 deg at a frequency of 51 Hz.

3.3. HC parameters

According to the analysis outlined in section 2.3, the HC applied for the main frequencies 3rd, 5th, and 7th is designed as follows:

− The compensator component targets the 3rd harmonic, resonating at frequency $3\omega_0$ (150 Hz) is designed with parameters including $\omega_c = 1$ rad/s and $K_{i3} = 500$;
− The compensator component targets the 5th harmonic, resonating at frequency $3\omega_0$ (150 Hz) is designed with parameters including $\omega_c = 1$ rad/s and $K_{i5} = 400$;
− The compensator component targets the 7th harmonic, resonating at frequency $3\omega_0$ (150 Hz) is designed with parameters including $\omega_c = 1$ rad/s and $K_{i7} = 300$;

The transfer function of the complete system with PR+HC (system in Figure 5) is presented as (10). Figures 8(a) and (b) respectively illustrate the bode diagram of its open-loop and closed-loop. By the function of MATLAB, the closed loop is determined to be stable with the gain margin obtained is 38.8 dB at 1210 Hz and the phase margin obtained is 13.8 deg at 151 Hz.

$$G_{PR}(s) + G_{HC}(s) = 10 + \frac{400s}{s^2+2s+(2\pi50)^2} + \frac{1000s}{s^2+2s+(2\pi150)^2} + \frac{800s}{s^2+2s+(2\pi250)^2} + \frac{1000s}{s^2+2s+(2\pi350)^2} \quad (10)$$
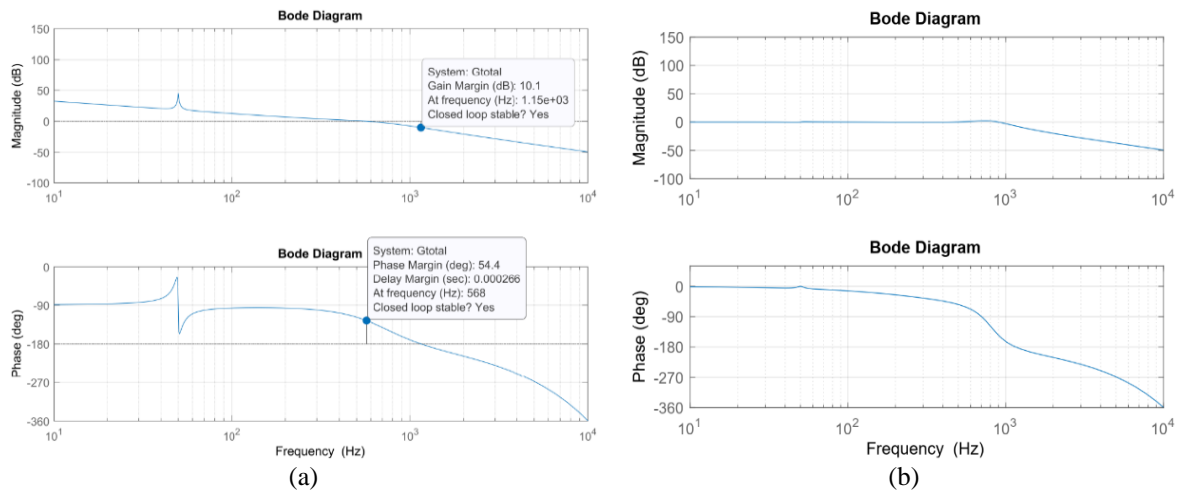

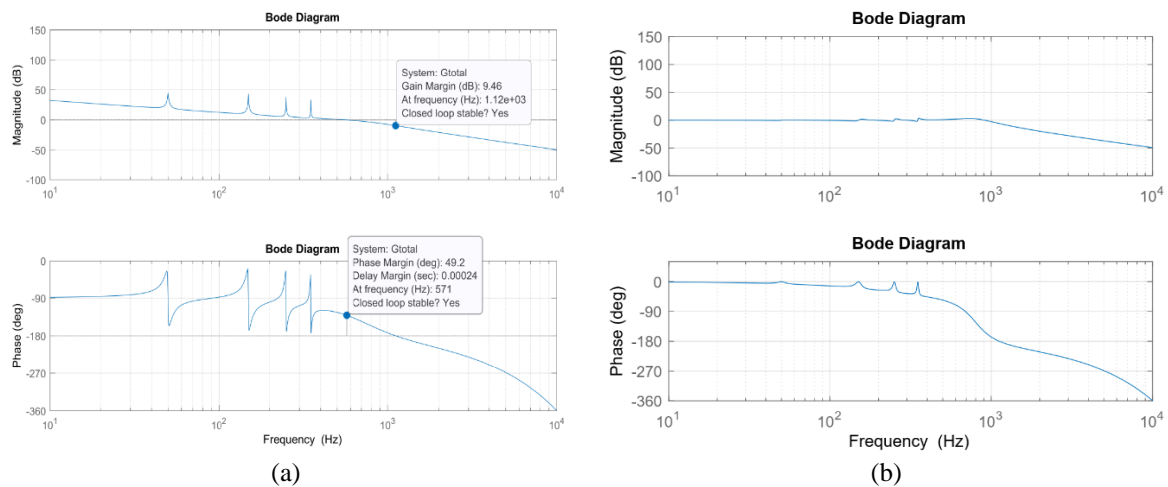Figure 7. Frequency responses of the system with PR controller without HC; (a) open-loop and (b) closed-loop

Figure 8. Frequency responses of the system with PR controller and HC; (a) open-loop and (b) closed-loop

4. SIMULATION RESULT

The 2 kWp PV inverter grid-connected with PR+HC system is modeled and simulated in MATLAB Simulink. The solar panel test parameters are placed under standard test conditions including 1000 W/m^2 radiation, 1.5 AM spectrum and a cell temperature of 25 °C. The study investigates the responsiveness of the PR+HC system in the case of grid voltage sinusoidal waveform with background THD=1.23%. The standard IEC 61727 [6] is used to evaluate the accuracy of the designed controller. Harmonic analysis using rectangular windows of 10 periods for 50 Hz networks (0.2 s with 5 Hz of resolution [4]). Total harmonic grid-current distortion is less than 5.0%; harmonic distortion ($h = 3,5,7$) is less than 4.0%. High-frequency harmonics from 9th and above are often lower than the standard, so they are not considered in the study. Simulations are performed to compare the effects of using and not using the HC system.

Figures 9(a) and (b) present the signal waveform for the two scenarios of the PR controller without and with the HC system, including the inverter current (I_i), grid current (I_g), reference current (I_{ref}), output voltage inverter (V_i), grid voltage (V_g), and DC voltage after the MPPT block (V_{dc}). There is no phase difference between the current and voltage signals in either simulation case. This demonstrates the effective function of the PR controller. Without the HC system, the odd harmonics produced by the inverter distort the current supplied to the grid, as shown in Figure 9(a). Due to the close resemblance between I_i and I_g, the LCL filter's performance is insufficient for filtering harmonics. When the PR controller is used with the HC system, there is a noticeable change in the current signal's smoothness. Standard sinusoidal waveform is shared by the current reference, the inverter current, and the grid current. This leads to the conclusion that the HC active filter outperforms the traditional LCL filter in terms of efficiency.
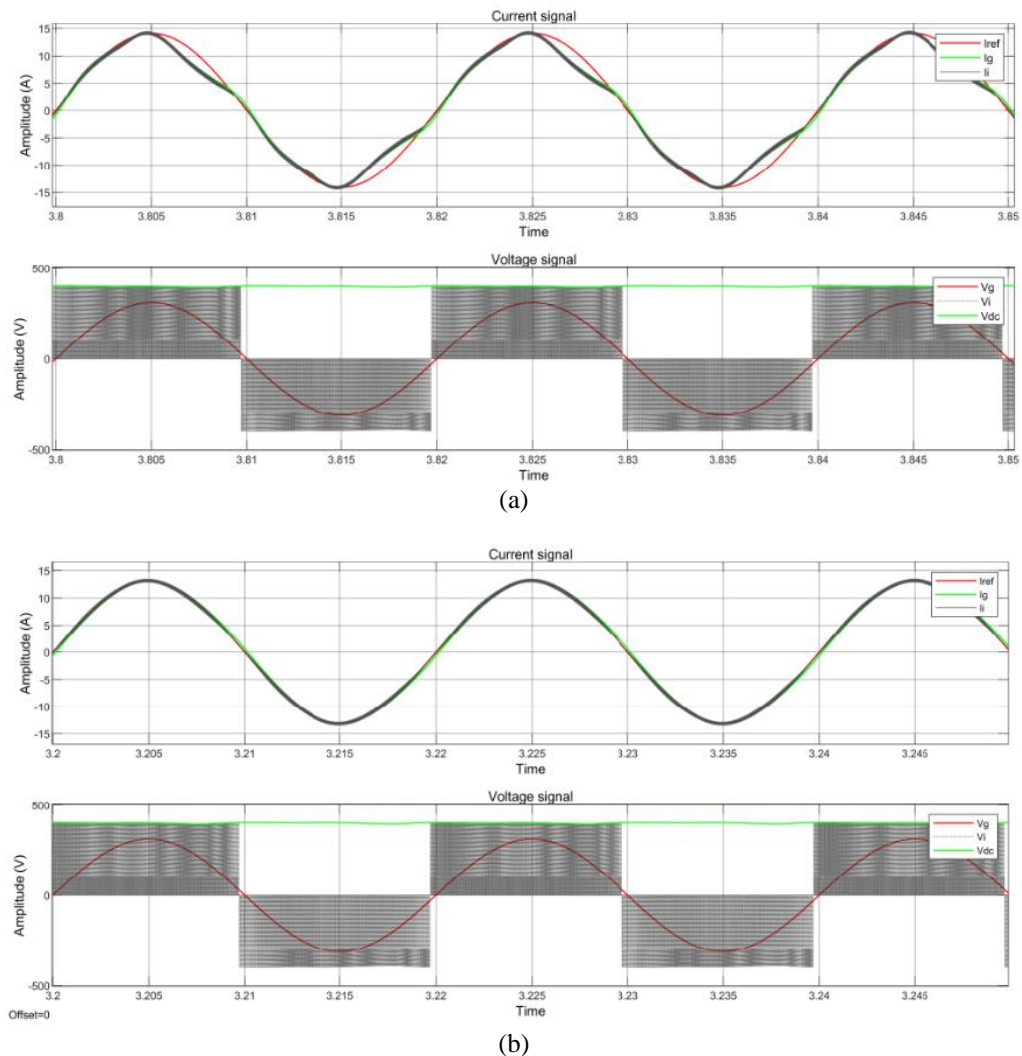

(a)

(b)

Figure 9. Simulation result of current waveform in two scenarios; (a) PR without HC and (b) PR with HC

MATLAB's FFT function is used to analyze the total harmonic current distortion. Figure 10 shows the THD result of each current harmonic of the inverter with PR controller in turn including Figure 10(a) without HC, Figure 10(b) with 3rd HC, Figure 10(c) with 3rd and 5th HC, and Figure 10(d) with 3rd, 5th, and 7th HC. Cases (a) and (d) are the two cases with the signals presented in Figures 9(a) and 9(b) respectively. Table 1 summarizes the harmonic amplitude values of the four cases mentioned above. In the case of using PR current controller without HC, THD has a high value of 8.81%, where 3rd and 5th harmonic did not meet IEC 61727 standard (7.42%>5% and 4.60%>4% respectively). The high frequency harmonics from 7th and above all meet the grid connection standard, less than 1%. The intensity of the frequency harmonics is minimized when applying the HC components to the PV inverter system in turn. THD value decreases from 8.81% to 1.03% and satisfies the requirement with THD limit of <5%. All odd harmonics of PV system have amplitude below 1%. The ability of harmonics reduction of each HC component is gradually reduced from 3rd HC to 3rd, 5th, 7th HC. For example, the 3rd HC has suppressed chiefly the amplitude of the 3rd and 5th harmonics, and they are already below the THD according to IEC 61727 standard (for 3rd harmonic, the amplitude drops from 7.42% to 1.92%; for 5th harmonic, the amplitude decreases from 4.60% to 2.93%). Although the 5th and 7th HC components also reduce the amplitude of the 250 Hz and 350 Hz harmonics, the attenuation is not much and has little effect on the 3rd harmonic. However, using a complete 3rd, 5th, and 7th HC unit is not redundant because the greater the reduction in harmonics, the more beneficial it is for the connected power grid.
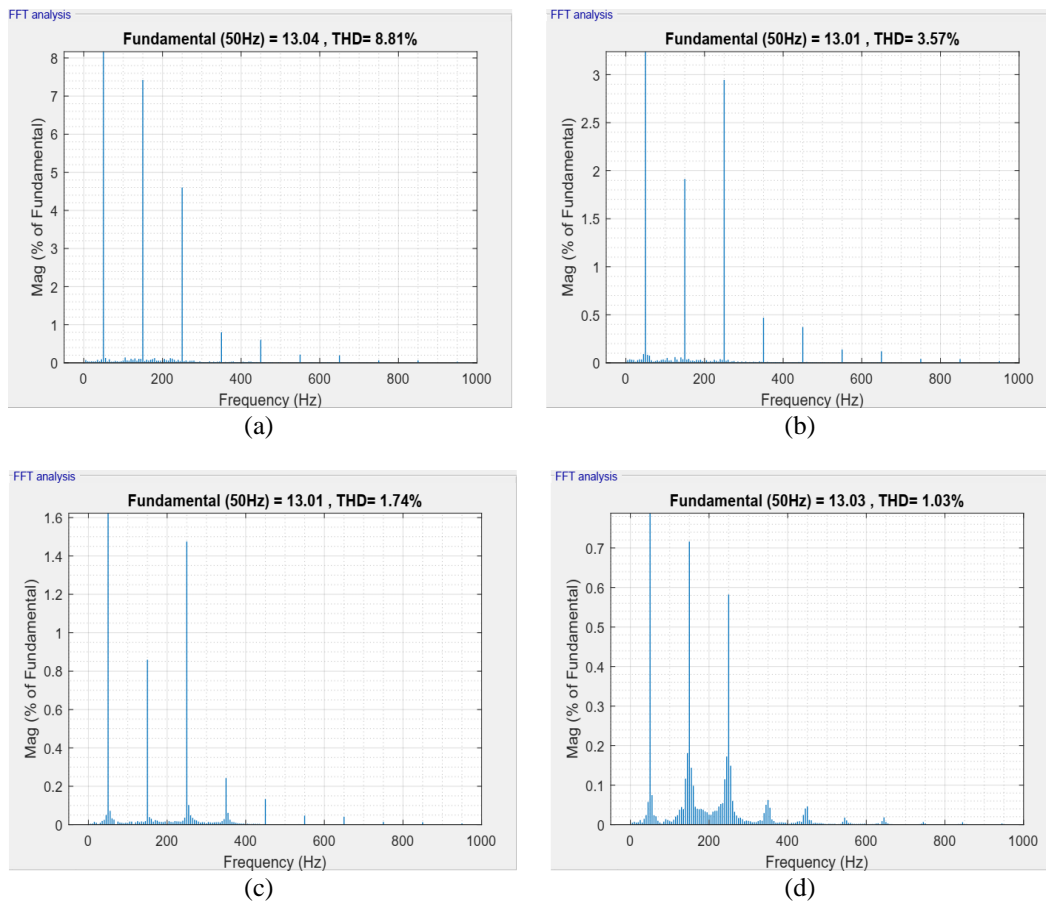

Figure 10. THD simulation results with 4 types of HC; (a) PR without HC, (b) PR with PR with 3rd HC, (c) PR with 3rd and 5th HC, and (d) PR with 3rd, 5th, and 7th HC

Table 1. Result of THD value of four case simulations

	THD (%)	1st harmonic (%)	3rd harmonic (%)	5th harmonic (%)	7th harmonic (%)
PR without HC	8.81	100	7.42	4.6	0.81
PR with 3rd HC	3.57	100	1.92	2.93	0.48
PR with 3rd and 5th HC	1.74	100	0.96	1.47	0.24
PR with 3rd, 5th, and 7th HC	1.03	100	0.72	0.58	0.06

In addition, the PR+HC system of PV inverter is also tested while the fluctuating grid frequency decreased to 49 Hz and increased to 51 Hz. Figure 11 shows the THD values of the grid current for two grid frequency variations: Figure 11(a) for $f_0 = 49$ Hz and Figure 11(b) for $f_0 = 51$ Hz. When the grid frequency changes, either up or down, THD slightly rises from 1.03% at $f_0 = 50$ Hz to 1.58% and 1.44% at $f_0 = 49$ Hz and $f_0 = 51$ Hz respectively. Each current harmonic's amplitude is under the IEC 61727 standard distortion limit. This indicates that the fundamental frequency fluctuations have relatively little impact on the PR+HC active filter.

| (a) | (b) |
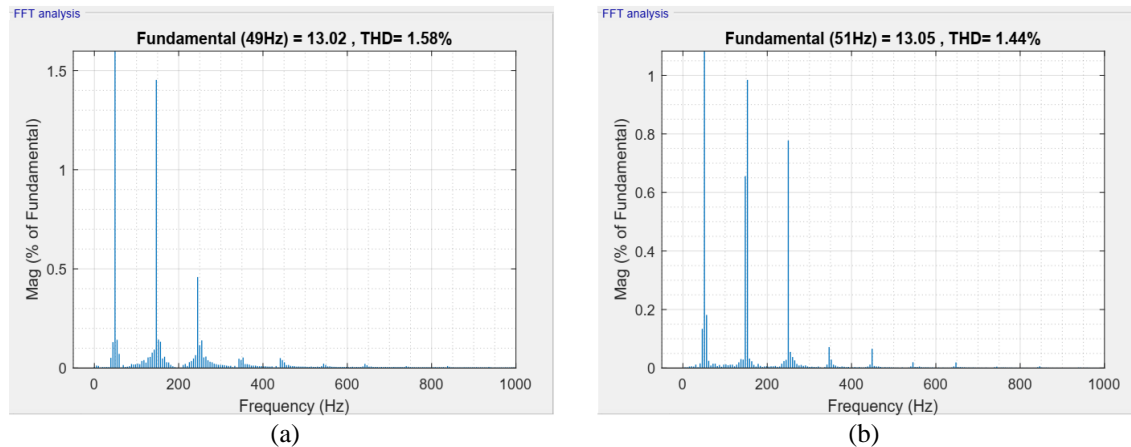
Figure 11. Simulation result of THD with PR+HC in case of grid frequency variation; (a) grid frequency $f_0 = 49$ Hz and (b) grid frequency $f_0 = 51$ Hz

5.   CONCLUSION

In this paper, a design of a PR current controller combined with HC active filter applied to a 2 kWp single-phase grid-connected PV is presented. This study also performed an analysis of the 3rd, 5th, and 7th frequency harmonic attenuating effectiveness of the HC system. Simulation results show the effectiveness of the PR+HC system in reducing the amplitude of the harmonics of 150 Hz, 250 Hz, and 350 Hz from 6.72%, 5.38%, and 1.15% of cases without HC to 0.72%, 0.58%, and 0.06%. The result meets the harmonic requirements of the PV inverter when synchronously connected to the power grid. In addition, the PR+HC system is stable and continues to function effectively when there is a fluctuation in the grid frequency in the range of 49 Hz to 51 Hz. In two fluctuating grid frequency scenarios, the THD value only slightly increased above the nominal frequency case. All of them have values below 2%. Through this study, applying the PR+HC system to each single PV installation can bring about an overall positive effect on the THD of a power grid. Ensuring each component lessens its harmonics can significantly improve the grid's overall operational efficiency. In the future, the research will conduct experimental tests on actual PV models and improve the integrated PR+HC unit for three-phase PV inverter as well as other types of DER.

REFERENCES

[1]   L. H. Lam, N. H. Hieu, and T. D. H. Phuc, "Simulation Models for Three-phase Grid-connected PV Inverters Enabling Current Limitation under Unbalanced Faults.," *Eng. Technol. Appl. Sci. Res.*, vol. 10, no. 2, 2020, doi: 10.48084/etasr.3343.
[2]   F. Blaabjerg, R. Teodorescu, M. Liserre, and A. V Timbus, "Overview of control and grid synchronization for distributed power generation systems," *IEEE Trans. Ind. Electron.*, vol. 53, no. 5, pp. 1398–1409, 2006, doi: 10.1109/TIE.2006.881997.
[3]   D. Obulesu and M. L. Swarupa, "Design of a novel control hysteresis algorithm for photovoltaic systems for harmonic compensation," *Bull. Electr. Eng. Inf.*, vol. 13, no. 1, pp. 31–37, 2024, doi: 10.11591/eei.v13i1.6038.
[4]   A. Arranz-Gimon, A. Zorita-Lamadrid, D. Morinigo-Sotelo, and O. Duque-Perez, "A review of total harmonic distortion factors for the measurement of harmonic and interharmonic pollution in modern power systems," *Energies*, vol. 14, no. 20, p. 6467, 2021, doi: 10.3390/en14206467.
[5]   T. Basso, "IEEE standard for interconnecting distributed resources with the electric power system," in *IEEE Pes Meeting*, 2004, p. 1.

[6]   I. E. Commission and others, "Characteristics of the utility interface for photovoltaic (PV) systems," *Rep. IEC*, vol. 61727, 2002.
[7]   K. Chahine, M. Tarnini, N. Moubayed, and A. El Ghaly, "Power Quality Enhancement of Grid-Connected Renewable Systems Using a Matrix-Pencil-Based Active Power Filter," *Sustain.*, vol. 15, no. 1, p. 887, 2023, doi: 10.3390/su15010887.
[8]   M. Bajaj, A. K. Singh, M. Alowaidi, N. K. Sharma, S. K. Sharma, and S. Mishra, "Power quality assessment of distorted distribution networks incorporating renewable distributed generation systems based on the analytic hierarchy process," *IEEE Access*, vol. 8, pp. 145713–145737, 2020, doi: 10.1109/ACCESS.2020.3014288.
[9]   V. Govindaraj, S. Mayakrishnan, S. Venkatarajan, R. Raman, and R. Sundar, "Design and development of photovoltaic solar system based single phase seven level inverter," *Bull. Electr. Eng. Inf.*, vol. 13, no. 1, pp. 58–66, 2024, doi: 10.11591/eei.v13i1.5168.
[10]   N. D. Tuyen, N. T. Thanh, V. X. S. Huu, and G. Fujita, "A combination of novel hybrid deep learning model and quantile regression for short-term deterministic and probabilistic PV maximum power forecasting," *IET Renew. Power Gener.*, vol. 17, no. 4, pp. 794–813, 2023.
[11]   A. P. S. Meliopoulos, F. Zhang, and S. Zelingher, "Power system harmonic state estimation," *IEEE Trans. Power Deliv.*, vol. 9, no. 3, pp. 1701–1709, 1994, doi: 10.1109/61.311191.
[12]   M. Digalovski, K. Najdenkoski, and G. Rafajlovski, "Impact of current high order harmonic to core losses of three-phase distribution transformer," in *Eurocon 2013*, 2013, pp. 1531–1535, doi: 10.1109/EUROCON.2013.6625181.
[13]   L. H. Lam and K. L. Nam, "A thorough comparison of optimization-based and stochastic methods for determining hosting capacity of low voltage distribution network," *Electr. Eng.*, 2023, doi: 10.1007/s00202-023-01985-2.
[14]   S. M. Ismael, S. H. E. A. Aleem, A. Y. Abdelaziz, and A. F. Zobaa, "State-of-the-art of hosting capacity in modern power systems with distributed generation," *Renew. energy*, vol. 130, pp. 1002–1020, 2019, doi: 10.1016/j.renene.2018.07.008.
[15]   L. H. Lam and K. L. Nam, "Developing Software to Evaluate the Ability of Distributed Energy Source Connected to the Distribution," *Meas. Control. Autom.*, vol. 3, no. 3, pp. 14–19, 2022.
[16]   R. F. Nadhim and A. K. Ibrahim, "Tuning proportional integral controller to enhance the photovoltaic system performance," *Bull. Electr. Eng. Inf.*, vol. 12, no. 6, pp. 3354–3364, 2023, doi: 10.11591/eei.v12i6.5337.
[17]   D. N. Zmood and D. G. Holmes, "Stationary frame current regulation of PWM inverters with zero steady-state error," *IEEE Trans. power Electron.*, vol. 18, no. 3, pp. 814–822, 2003.
[18]   R. Teodorescu, F. Blaabjerg, M. Liserre, and P. C. Loh, "Proportional-resonant controllers and filters for grid-connected voltage-source converters," *IEE Proceedings-Electric Power Appl.*, vol. 153, no. 5, pp. 750–762, 2006, doi: 10.1049/ip-epa:20060008.
[19]   B. Li, W. Yao, L. Hang, and L. M. Tolbert, "Robust proportional resonant regulator for grid-connected voltage source inverter (VSI) using direct pole placement design method," *IET Power Electron.*, vol. 5, no. 8, pp. 1367–1373, 2012, doi: 10.1049/iet-pel.2012.0102.
[20]   D. Pérez-Estévez, J. Doval-Gandoy, A. G. Yepes, Ó. López, and F. Baneira, "Enhanced resonant current controller for grid-connected converters with LCL filter," *IEEE Trans. Power Electron.*, vol. 33, no. 5, pp. 3765–3778, 2017, doi: 10.1109/TPEL.2017.2770218.
[21]   L. Herman, I. Papic, and B. Blazic, "A proportional-resonant current controller for selective harmonic compensation in a hybrid active power filter," *IEEE Trans. power Deliv.*, vol. 29, no. 5, pp. 2055–2065, 2014, doi: 10.1109/TPWRD.2014.2344770.
[22]   G. Shen, X. Zhu, J. Zhang, and D. Xu, "A new feedback method for PR current control of LCL-filter-based grid-connected inverter," *IEEE Trans. Ind. Electron.*, vol. 57, no. 6, pp. 2033–2041, 2010.
[23]   M. Parvez, M. F. M. Elias, N. Abd Rahim, F. Blaabjerg, D. Abbott, and S. F. Al-Sarawi, "Comparative study of discrete PI and PR controls for single-phase UPS inverter," *IEEE Access*, vol. 8, pp. 45584–45595, 2020, doi: 10.1109/ACCESS.2020.2964603.
[24]   D. Zammit, M. Apap, and C. Spiteri Staines, "Comparison between PI and PR current controllers in grid connected PV inverters," *Int. J. Electr. Comput. Eng.*, vol. 8, no. 2, pp. 221-226, 2014.
[25]   M. Parvez, M. F. M. Elias, and N. A. Rahim, "Performance analysis of PR current controller for single-phase inverters," *IET Clean Energy Technol. Conf.*, Kuala Lumpur, Malaysia, 2016, pp. 1-8, doi: 10.1049/cp.2016.1311.
[26]   M. Castilla, J. Miret, J. Matas, L. G. de Vicuña, and J. M. Guerrero, "Linear current control scheme with series resonant harmonic compensator for single-phase grid-connected photovoltaic inverters," *IEEE Trans. Ind. Electron.*, vol. 55, no. 7, pp. 2724–2733, 2008, doi: 10.1109/TIE.2008.920585.
[27]   M. Castilla, J. Miret, J. Matas, L. G. De Vicuña, and J. M. Guerrero, "Control design guidelines for single-phase grid-connected photovoltaic inverters with damped resonant harmonic compensators," *IEEE Trans. Ind. Electron.*, vol. 56, no. 11, pp. 4492–4501, 2009, doi: 10.1109/TIE.2009.2017820.
[28]   M. Y. Ali Khan, H. Liu, Z. Yang, and X. Yuan, "A comprehensive review on grid connected photovoltaic inverters, their modulation techniques, and control strategies," *Energies*, vol. 13, no. 16, p. 4185, 2020, doi: 10.3390/en13164185.
[29]   S. T. Y. Alfalahi *et al.*, "Supraharmonics in power grid: Identification, standards, and measurement techniques," *IEEE Access*, vol. 9, pp. 103677–103690, 2021, doi: 10.1109/ACCESS.2021.3099013.
[30]   A. Kalair, N. Abas, A. R. Kalair, Z. Saleem, and N. Khan, "Review of harmonic analysis, modeling and mitigation techniques," *Renew. Sustain. Energy Rev.*, vol. 78, pp. 1152–1187, 2017, doi: 10.1016/j.rser.2017.04.121.
[31]   P. Mattavelli, "A closed-loop selective harmonic compensation for active filters," *IEEE Trans. Ind. Appl.*, vol. 37, no. 1, pp. 81–89, 2001, doi: 10.1109/28.903130.
[32]   P. Karuppanan and K. K. Mahapatra, "Active harmonic current compensation to enhance power quality," *Int. J. Electr. Power Energy Syst.*, vol. 62, pp. 144–151, 2014, doi: 10.1016/j.ijepes.2014.04.018.
[33]   J. He, Y. W. Li, F. Blaabjerg, and X. Wang, "Active harmonic filtering using current-controlled, grid-connected DG units with closed-loop power control," *IEEE Trans. Power Electron.*, vol. 29, no. 2, pp. 642–653, 2013, doi: 10.1109/TPEL.2013.2255895.
[34]   S. U. Islam *et al.*, "Design of a proportional resonant controller with resonant harmonic compensator and fault ride trough strategies for a grid-connected photovoltaic system," *Electronics*, vol. 7, no. 12, p. 451, 2018.
[35]   D. Zammit, C. S. Staines, M. Apap, and J. Licari, "Design of PR current control with selective harmonic compensators using Matlab," *J. Electr. Syst. Inf. Technol.*, vol. 4, no. 3, pp. 347–358, 2017, doi: 10.1016/j.jesit.2017.01.003.
[36]   D. Kumar and F. Zare, "Harmonic analysis of grid connected power electronic systems in low voltage distribution networks," *IEEE J. Emerg. Sel. Top. Power Electron.*, vol. 4, no. 1, pp. 70–79, 2015, doi: 10.1109/JESTPE.2015.2454537.

BIOGRAPHIES OF AUTHORS

Le Khoa Nam received a bachelor's in electrical engineering from The University of Danang-University of Science and Technology, Vietnam, 2021. His main research interests include power system operation optimization, renewable energy, distributed energy resource, and protection relay. He can be contact at email: 105170040@sv1.dut.udn.vn.

Le Hong Lam received a Ph.D. in electrical engineering from Politecnico di Milano, Milan, Italy, 2017. During the period from February 2018 to February 2019, he worked at the Department of Energy at Politecnico di Milano with a postdoctoral research position. He is currently a Senior lecturer at the Faculty of Electrical Engineering the University of Danang University of Science and Technology, Vietnam. His research interests include the integration of renewable energy sources into the grid, electricity markets, and power system planning. He can be contacted at email: lhlam@dut.udn.vn.

Trinh Trung Hieu received the Ph.D. degree in electrical engineering from the Grenoble Institute of Technology, France, in 2013. He became a professor at Danang University of Science and Technology, Vietnam, in 2013. Since 2015 he is head of Power System Department at the Faculty of Electrical Engineering - The University of Danang-University of Science and Technology, Vietnam. His main research interests are in power electronics, micro converter networks, and hybrid integration. He can be contacted at email: tthieu@dut.udn.vn.

Nguyen Huu Hieu received his Ph.D. degree in electrical engineering from the University of Joseph Fourier, Grenoble, France, in 2008. Since 2010, he is a Senior Lecturer at the Faculty of Electrical Engineering, The University of Danang–University of Science and Technology, Danang, Vietnam. He was a Post-Doctoral Researcher with the Grenoble Institute of Technology, Grenoble, France, as part of the G2ELab in 2008-2010. Since 2018, he has been an associate professor of electric power systems. He is currently Rector of The University of Danang-University of Science and Technology, Vietnam. His research interests include optimization in power systems, power quality, and distributed energy resources. He can be contacted at email: nhhieu@dut.udn.vn.